Onset of multifragmentation in intermediate energy light asymmetrical collisions

Y. G. Ma and W. Q. Shen
*China Center of Advanced Science and Technology (World Laboratory), P.O. Box 8730, Beijing 100080, China and Institute of Nuclear Research, Academia Sinica, P.O. Box 800-204, Shanghai 201800, China**
(Received 6 May 1994)

The multifragment emission for central collisions of ^{40}Ar(25–150 MeV/nucleon) on ^{27}Al was studied via the quantum molecular dynamics model. The distribution of intermediate mass fragments (IMF's) can be described by a power-law function with the parameter τ or an exponential function with the parameter λ. By increasing the beam energy, the mean multiplicity of IMF's and relative cross sections for emitting multifragments first increase to their maximum values and then decrease; while the extracted τ, λ parameters and relative cross section for single IMF emission show the converse tendency. The calculation and relevant experiment suggest that the reactions have a critical energy point where the onset of multifragmentation takes place.

PACS number(s): 25.70.Pq, 24.60.Ky

The emission of intermediate mass fragments ($3 \leq Z \leq Z_{\text{total}}/3$) is an important probe of the dynamical evolution in intermediate energy (20–1000 MeV/nucleon) heavy-ion collisions. At low energies (<20 MeV/nucleon) intermediate mass fragment (IMF) emission is a rare process while at high energies (> several GeV/nucleon) the reaction is so violent for central collisions that the system disassembles into nucleons, pions, and light fragments like α particles. In the transition region, multifragment emission, which is defined such that final states involve two or more IMF's [1,2], has been experimentally observed [3–13]. With increasing excitation energy one may expect a rise and fall of multifragment emission [6]. However, the dominant mechanism of multifragment emission has not yet been unambiguously determined. On the other hand, the liquid-gas phase transition in infinite nuclear matter has been predicted to occur at intermediate energy [14–16] and it may be related to multifragment emission [17]. The measured inclusive charge distribution of fragments on multifragmentation from proton-induced reactions displayed a minimum for the power-law parameter τ of charge distribution ($\sigma \propto Z^{-\tau}$) as a function of beam energy, which was interpreted as evidence for the liquid-gas phase transition [18]. However, this interpretation is disputed, partly since the authors made no selection on the impact parameter. In this article we study the fragment mass distribution of central collisions for ^{40}Ar on ^{27}Al from 25 to 150 MeV/nucleon and report that there unambiguously exists a turning point of multifragment emission via many-body correlation theory—the quantum molecular dynamics (QMD) approach, which may be related to the liquid-gas phase transition in nuclear matter with the finite-size effect of the reaction.

In view of the experimental results on fragment emission, various theoretical models embodying different decay mechanisms have been developed. These models can be more or less divided into two classes: statistical and dynamical models [16,19]. Statistical models range from a standard sequential-statistical binary decay model to a simultaneous multifragment decay model. Dynamical models range from nuclear shattering to spinodal instability. Of the dynamical models, the quantum molecular dynamics approach, one of the many-body correlation transport theories, has been extensively used to describe the production of IMF's [20]. In addition, percolation models and hybrid approaches have also been used to discuss the fragment emission. However, up to date, detailed model calculations on the excitation function of multifragment emission and prediction of the critical energy of multifragmentation are still rare, especially with dynamical models.

The QMD model explicitly treats the nucleon correlation information through the time evolution of the collision; it is able to describe the fluctuations that lead to the final fragmentation of the nuclear system. This is a major improvement over the mean-field models, which can describe only average properties of the collisions and do not contain the explicit correlations necessary to create IMF's. In the QMD model each nucleon is represented by a Gaussian wave packet with a width $\sqrt{L}$ centered around the mean position $\vec{r}_j(t)$ and the mean momentum $\vec{p}_j(t)$,

$$\psi_j(\vec{r},t) = \frac{1}{(2\pi L)^{3/4}} \exp\left[\frac{-[\vec{r}-\vec{r}_j(t)]^2}{4L}\right] \times \exp\left[\frac{-i\vec{p}_j(t)\cdot\vec{r}}{\hbar}\right].$$

The nucleons interact via potential and collisions. The long-range Coulomb force and Yukawa interactions are also included. The time evolution of the Gaussians is given by the generalized variational principle. Details may be found in Ref. [20]. In this work, we simulate the central collisions of ^{40}Ar+^{27}Al on an event-by-event basis with the QMD model. We use the momentum-independent Skyrme-type effective interaction and take the parameters corresponding to the hard equation of state (EOS) with incompressibility $K = 380$ MeV. The

*Mailing address.

free nucleon-nucleon (N-N) cross sections are modified in the nuclear medium by the Uehling-Ulenbeck blocking factor, which determines the Pauli blocking probability of the final states in N-N collisions.

Before using the QMD approach to treat the production of IMF's, we would like to point out some viewpoints on the application of dynamical models like QMD in fragment emission. On the one hand, the normal QMD approach does not provide genuine ground states and thus has small spurious nucleon emission [21–23]. The Kyoto group has developed a collisional cooling method in the initialization of collisions of two nuclei; it can construct very stable nuclei and there is no spurious nucleon evaporation during a period of more than 1000 fm/c, which will be especially important if one treats low energy collisions with the molecular dynamical model [23]. In this work, we checked the initial configurations of nuclei and spurious nucleon emission, and found they do not influence our studies on multifragmentation as stated here. Dynamical models like QMD have also been thought to have difficulties at a later stage of the reaction because the final primary fragments via the QMD calculation may be very excited; they can deexcite still further via evaporation. So some hybrid approaches, such as dynamics followed by statistical decay [24–26], or by using the restricted aggregation model [22,27] and evaporation occurring simultaneously with dynamical expansion [28], were used to fit the fragment yield quantitatively. Conversely, Müller *et al.* point out that there is no need to supplement the QMD calculation by an additional evaporation model in treating the deexcitation process of single excited nuclei. Due to the fragment emission pattern in QMD, governed by phase space as in statistical models, Müller *et al.* thought that the differences between the QMD results and the data are not due to insufficiencies in the description of the excited system, but instead are probably due to an unsuitable free cross section in the nuclear environment and/or a lack of energy deposition in the spectator matter [29]. Irregardless, the predicted distributions of IMF's via QMD directly have at least a similar shape to experimental data, but some discrepancy of yield may exist between the data and calculations; however, this discrepancy should not change the energy dependence of the multifragment emission. Moreover, in our opinion, the hybrid models are still, to some extent, in an arbitrary stage. On the one hand, when the dynamical process should switch off and the excited system then be treated with a statistical model is still not clearly determined, and, on the other hand treatments with different statistical models may result in different final fragments. Since we mainly investigate the physics from the energy dependence of the multifragment emission rather than by quantitative comparison to data in this article, we can directly simulate the production of IMF's via the QMD model.

In our simulation, we defined the fragments to have been created as the centroids of wave packets of two nucleons having a spatial distance $d_0 \leq 3$ fm (a change of d_0 does not influence the fragment yields sensitively) [21]. In order to get a reasonable extracted time of fragment emission, we studied in detail the formation history of nucleons and fragments in different mass bins and found that the IMF is sufficiently stable after 120–140 fm/c and heavy fragments ($A \geq 23$) do not decay further after 80–100 fm/c. We also found that nucleon emission at later stages stems mainly from the unstable light fragments ($2 \leq A \leq 4$) [30]. So we may extract the IMF around 120 fm/c and sum over the fragment yield from 140 to 200 fm/c to plot the succeeding fragment mass distribution in order to get good fits to IMF distributions.

In Fig. 1 the calculated mass distributions for central collisions of ^{40}Ar+^{27}Al at $b = 0$ and 2.5 fm are shown as a function of the beam energy. The circles with bar show the final fragment yield and the curves indicate the power-law fits of $\sigma(A) \propto A^{-\tau}$ for IMF's ($5 \leq A \leq 22$). In addition, the exponential fits of $\sigma(A) \propto e^{-\lambda A}$ for the IMF's have also been made as in Ref. [11]. We found that both fit forms are suitable for the IMF's from central collisions in all energies addressed here. Clearly, the range of mass distribution becomes narrow with increasing beam

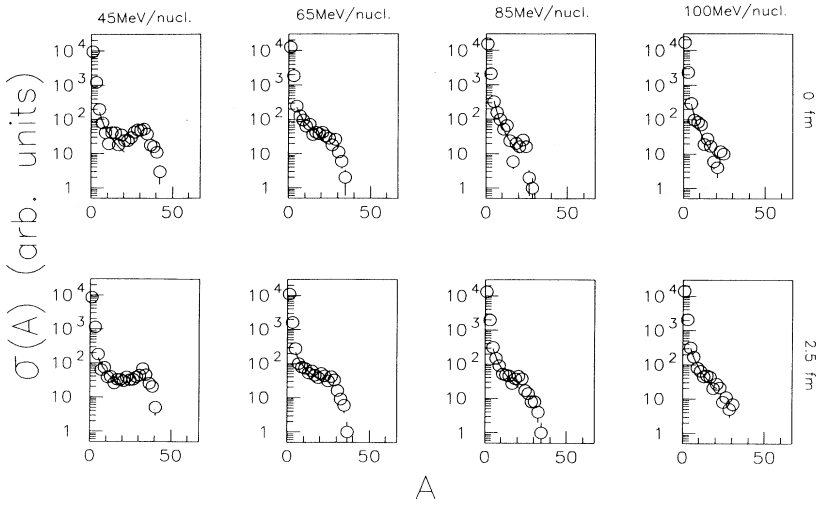

FIG. 1. The fragment mass distributions of ^{40}Ar+^{27}Al at beam energies of 45, 65, 85, and 100 MeV/nucleon for $b = 0$ fm (top row) and for $b = 2.5$ fm (bottom row). The circles show the calculated results via QMD and the curves represent the power-law fits of mass distribution for IMF's ($5 \leq A \leq 22$). The unit of $\sigma(A)$ is arbitrary.

energy and impact parameter, which reflects the increase of violence of collisions. Below 65 MeV/nucleon, a large-mass residue survives while for collisions above 65 MeV/nucleon the reactions produce many light particles and IMF's. Increasing beam energy, the distributions of IMF's become less steep from lower energy, 25 MeV/nucleon, to medium energy, 65 MeV/nucleon. This implies that the reactions below 65 MeV/nucleon are characteristic of light-fragment evaporation from a heavy system, and this feature shows most clearly at the lowest energy (25 MeV/nucleon) due to the formation of less lower excited nuclei closer to equilibrium. For collisions above 65 MeV/nucleon, the distributions of IMF's become steep with increasing beam energy because the system disintegrates into fragments more completely at high energies. If we consider the phase space distribution, they can be clearly distinguished. Figure 2 plots the particle distribution from the side view (X-Z plane) and front view (X-Y plane) in coordinate space around 65 MeV/nucleon (extracted around 200 fm/c). Obviously, in the 45 MeV/nucleon case, a heavy remnant remains and many light particles and small IMF's are produced together; while in the 85 MeV/nucleon case, the system seems to undergo a multifragmentation. Between both cases, a critical region can be found around 65 MeV/nucleon, where the system has very large expansion and shows a rather loose structure of nuclei, and will be highly unstable in further time evolution.

This kind of evolution of the reaction mechanism can be seen more clearly from the rise and fall of some observables of IMF's in Fig. 3. Figure 3(a) shows the excitation function of extracted τ and λ parameters. Obviously, the minimum values of τ around 1.6 and λ around 0.15 at 65 MeV/nucleon are observed for both cases at $b = 0$ and 2.5 fm. At both sides of this energy, the τ and λ values seem to be rather sensitive to the centrality of the collisions. Such kind of sensitivity of τ or λ to the impact parameter b at different energies may provide additional evidence for critical behavior, say, e.g., the liquid-gas phase transition. Figures 3(b) and 3(c) depict the excitation function of the mean multiplicity of IMF's ($\langle$IMF$\rangle$) and of relative cross sections producing 1–4 IMF's ($\sigma_{\rm IMF}$). Again, a critical point occurs around 65 MeV/nucleon for $\langle$IMF$\rangle$ and $\sigma_{\rm IMF}$. At the lower energies the system emits fewer IMF's and produces larger-mass liquid condensed clusters due to evaporation, while for higher energies the system disassembles into smaller particles and the multiplicity of IMF's decreases due to nuclear vaporization. Around 65 MeV/nucleon at $b = 0$ and 2.5 fm, the maximum $\langle$IMF$\rangle$ reaches to ~ 2 and the maximum multiplicity can rise to 6–7 and insensitivity to the impact parameter is also found again. For central collisions above 90 MeV/nucleon, the impact parameter dependence of $\langle$IMF$\rangle$ is qualitatively similar to the cases of 600 MeV/nucleon Au on Al and Cu [6]. It is worthwhile noting that $\sigma_{\rm IMF=1}$ of single IMF events has a minimum around 65 MeV/nucleon; this also may be a signal of a critical point occurring there. For the multiple IMF events, the relative cross section generally shows a steep increase up to 65 MeV/nucleon, becomes an approximate plateau, and then decreases. In a previous experimental report for the central collisions of ^{40}Ar on ^{27}Al measured via 4π detectors [31], the authors presented a picture like our Fig. 3(c) but only below 65 MeV/nucleon, due to the insufficient statistics and the lack of measurements at higher energies at that time. Similar trends of the excitation function for $\sigma_{\rm IMF=1}$ and $\sigma_{\rm IMF\geq 2}$ were observed experimentally below 65 MeV/nucleon. Of course, the calculated results should be filtered by the detector acceptance if quantitative comparison between the experiment and the theory is made.

Figure 4 shows $\ln(M_{\rm max})$ for the largest fragment per event plotted vs $\ln(S2)$ of the normalized second moment of the fragment distribution for one event with the largest fragment excluded, where

$$S2 = \frac{\sum_{i,A\neq M_{\rm max}} A_i^2 n_i(A_i)}{\sum_{i,A\neq M_{\rm max}} A_i n_i(A_i)},$$

i.e., the so called Campi scatter plot [32], at different en-

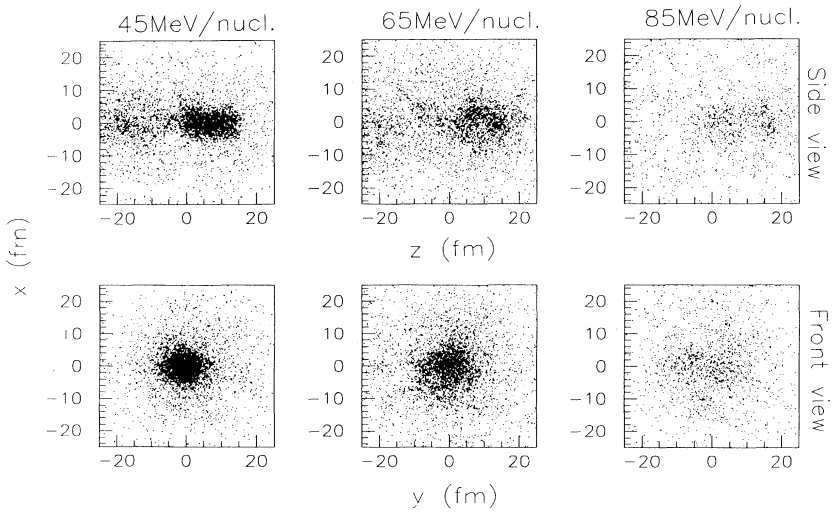

FIG. 2. The final-state particle distribution in the X-Z plane (top row) and in the X-Y plane (bottom row) for 45 MeV/nucleon (left), 65 MeV/nucleon (middle), and 85 MeV/nucleon (right) at $b = 0$ fm. All units of coordinates are in fm.

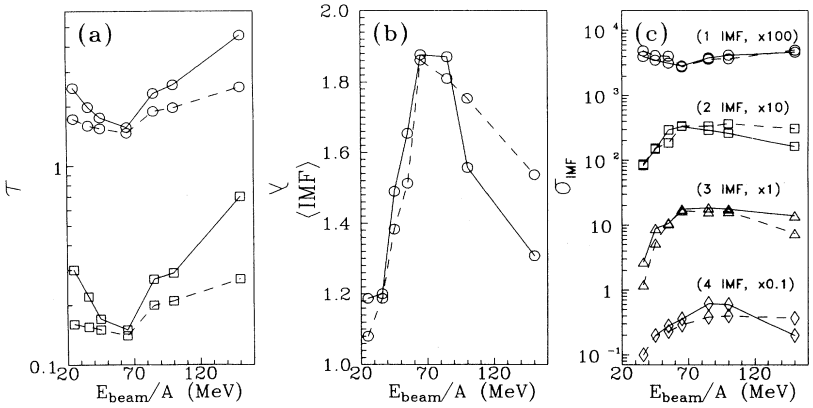

FIG. 3. The τ and λ parameters extracted by the fit of IMF mass distribution (a), the average IMF multiplicity (b), and the relative cross section producing 1–4 IMF's (c) are plotted as a function of the beam energy for the ^{40}Ar+^{27}Al reaction system. The solid line and dashed line correspond to the cases of $b = 0$ and 2.5 fm, respectively. In (a) circles and squares stand for the τ and λ parameter, respectively. In (c) $\sigma_{\rm IMF}$ has arbitrary units.

ergies. Around 65 MeV/nucleon the plot clearly shows two different branches: one branch at larger $M_{\rm max}$ comes from an undercritical state and the other at smaller $M_{\rm max}$ from a supercritical state due to a possible liquid-gas coexistence phase. At lower energies like 36 MeV/nucleon, the plot shows only the undercritical branch where the fragment emission is sequential; the heavy fragments may correspond to the liquid condensed phase. At higher energies like 100 MeV/nucleon, the plot shows mainly the supercritical branch where vaporization may take place in the system and the fragments result from simultaneous breakup of the system. In addition, we also found that the average largest fragment $\langle M_{\rm max}\rangle$ in the events starts to be smaller than 22, which is the highest value of IMF's for central collisions at 65 MeV/nucleon.

In terms of the descriptions above, the turning point can be well defined around 65 MeV/nucleon for the reaction addressed here. Around 65 MeV/nucleon, the reaction shows minima for τ, λ, and $\sigma_{\rm IMF=1}$ while there are maxima for $\langle$IMF$\rangle$ and $\sigma_{\rm IMF\geq 2}$. A similar observation of τ parameter versus apparent temperature has been made where the authors interpreted the minimum τ as evidence of the liquid-gas phase transition [33]. Recently reported experimental results of Au-induced multifragmentation also show similar phenomena for the deposited energy dependence of τ and $\langle$IMF$\rangle$ [6]. Ar-induced symmetrical reactions (^{40}Ar+^{45}Sc) from 35 to 115 MeV/nucleon combined with the Au-induced data given qualitative agreement with our results [11]. Our turning energy of 65 MeV/nucleon corresponds to an excitation energy of about 5.5 MeV/nucleon, considering preequilibrium emission and neutron correction [34], which have just exceeded the estimated threshold for multifragmentation, about $E^*/A \sim 5$ MeV [10,35]. We therefore think that the onset of multifragmentation for central ^{40}Ar on ^{27}Al collisions takes place around 65 MeV/nucleon and it may correspond to the liquid-gas phase transition with the finite-size effect correction. Below that energy fragment emission is sequential and rare since the system is undercritcal and above it the fragments stem from multifragmentation since the system is supercritical. In comparison with other experimental data, our results also seem to be reasonable. For the nearly symmetrical collision of Ar on Sc, the critical point occurs around 35 MeV/nucleon [11] while for slightly asymmetrical Ar on V collisions it takes place at 45–65 MeV/nucleon [36]. Another experiment of Kr+Nb also suggests 55 MeV/nucleon as a critical energy for the onset of multifragmentation via the IMF-IMF correlation method [37].

In summary, we have investigated the production of fragments ($5 \leq A \leq 22$) from central collisions for ^{40}Ar (25–150 MeV/nucleon) on ^{27}Al via the molecular dynamical model. We observed that there exists a turning point around 65 MeV/nucleon. This critical point may manifest the following behaviors: (1) a minimum for the power-law parameter τ (or exponential parameter λ) for the distributions of IMF's; (2) a minimum for the relative cross section producing a single IMF; (3) a maximum for the average multiplicity of IMF's; (4) maxima for the relative cross section producing multiple IMF's.

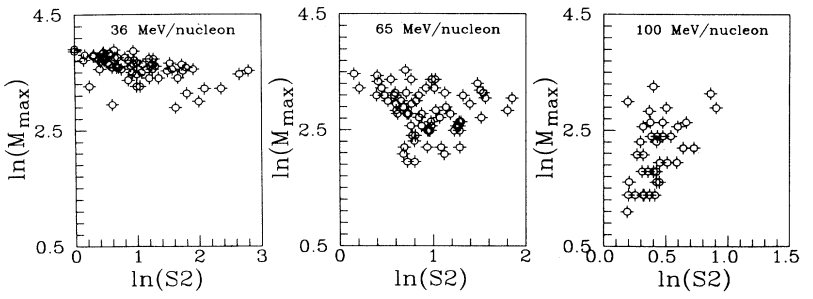

FIG. 4. The Campi scatter plots for 36, 65, and 100 MeV/nucleon ^{40}Ar+^{27}Al at $b = 0$ fm.

Of course, the above points considered as a manifestation of a critical point are correlated with each other to some extent, in particular for small systems [38]. We also show the final-state X-Z and X-Y space distributions of particles around this critical energy; it is clearly seen that above this energy the system undergoes multifragmentation and below it a heavy remnant survives and fragments stem mainly from evaporation. Experimental analysis for the same system gives an excitation energy of 5.5 MeV/nucleon at 65 MeV/nucleon, which is just larger than the estimated threshold for multifragmentation. Moreover, the Campi scatter plot shows clearly the undercritical and supercritical branches simultaneously at 65 MeV/nucleon which may reflect liquid-gas coexistence. Combining the above characteristics, we conclude that the turning point around 65 MeV/nucleon corresponds to the onset of multifragmentation and may relate to the nuclear liquid-vapor phase transition in finite nuclear matter. In addition, we observe an insensitivity of the τ (or λ) parameter and of the average IMF multiplicity to the impact parameter in a certain range of central collisions at the critical energy. Is this a curious coincidence or an indication of the liquid-gas phase transition? We prefer the latter. Of course, further evidence of the liquid-gas phase transition in intermediate energy nuclear systems is needed both experimentally and theoretically. A knowledge of the EOS may also be obtained from the comparison of the experimental excitation function for multifragment emission with the calculations. Systematic studies of the dependence of multifragment emission on the system mass and its asymmetry are, of course, very interesting for both experiments and theories.

This work is supported partly under NNSF of China.

[1] W. G. Lynch, Annu. Rev. Nucl. Part. Sci. **37**, 493 (1987).
[2] D. H. E. Gross, Rep. Prog. Phys. **53**, 605 (1990).
[3] A. I. Warwick, H. H. Wieman, H. H. Gutbrod, M. R. Maier, J. Péter, H. G. Riter, H. Stelzer, F. Weik, M. Freedman, D. J. Henderson, S. B. Kaufman, E. P. Steinberg, and B. D. Wilkins, Phys. Rev. C **27**, 1083 (1983).
[4] Y. D. Kim, M. B. Tsang, C. K. Gelbke, W. G. Lynch, N. Carlin, Z. Chen, R. Fox, W. G. Gong, T. Muakami, T. K. Nayak, R. M. Ronningen, H. M. Xu, F. Zhu, W. Bauer, L. G. Sobotka, D. Stracener, D. G. Sarantities, Z. Majka, V. Abenante, and H. Griffin, Phys. Rev. Lett. **63**, 494 (1989).
[5] S. J. Yellenno, E. C. Pollacco, K. Kwiatkowski, C. Volant, R. Dayras, Y. Cassagnou, R. Legrain, E. Norbeck, V. E. Viola, J. L. Wile, and N. R. Yoder, Phys. Rev. Lett. **67**, 671 (1991); S. J. Yellenno, K. Kwiatkowski, E. C. Pollacco, C. Volant, Y. Cassagnou, R. Dayras, D. E. Fields, S. Harar, E. Hourani, R. Legrain, E. Norbeck, R. Planeta, J. L. Wile, N. R. Yoder, and V. E. Viola, Phys. Rev. C **48**, 1092 (1993).
[6] C. A. Ogilvie, J. C. Adolff, M. Begemann-Blaich, P. Bouissou, J. Hubele, G. Imme, I. Iori, P. Kreutz, G. J. Kunde, S. Leray, V. Lindenstruth, Z. Liu, U. Lynen, R. J. Meijer, U. Milkau, W. F. J. Müller, C. Ngô, J. Pochodzalla, G. Raciti, G. Rudolf, H. Sann, A. Schüttauf, W. Seidel, L. Stuttge, W. Trautmann, and A. Tucholski, Phys. Rev. Lett. **67**, 1214 (1991).
[7] D. R. Bowman, G. F. Peaslee, R. T. de Souza, N. Carlin, C. K. Gelbke, W. G. Gong, Y. D. Kim, M. A. Lisa, W. G. Lynch, L. Phair, M. B. Tsang, C. Williams, N. Colonna, K. Hanold, M. A. McMahan, G. J. Wozniak, L. G. Moretto, and W. A. Friedman, Phys. Rev. Lett. **67**, 1527 (1991).
[8] R. T. de Souza, L. Phair, D. R. Bowman, N. Carlin, C. K. Gelbke, W. G. Gong, Y. D. Kim, M. A. Lisa, W. G. Lynch, G. F. Peaslee, M. B. Tsang, H. M. Xu, and F. Zhu, Phys. Lett. B **268**, 6 (1991).
[9] K. Hagel, M. Gonin, R. Wada, J. B. Natowitz, B. H. Sa, Y. Lou, M. Gui, D. Utley, G. Nebbia, D. Fabris, G. Prete, J. Ruiz, D. Drain, B. Chambon, B. Cheynis, D. Guinet, X. C. Hu, A. Demeyer, C. Pastor, A. Giorni, A. Lleres, P. Stassi, J. B. Viano, and P. Gonthier, Phys. Rev. Lett. **68**, 214 (1992).
[10] J. B. Natowitz *et al.*, Nucl. Phys. A **538**, 263c (1992).
[11] T. Li, W. Bauer, D. Craig, M. Cronqvist, E. Gualtieri, S. Hannuschke, R. Lacey, W. J. Llope, T. Reposeur, A. M. Vander Molen, G. D. Westfall, W. K. Wilson, J. S. Winfield, J. Yee, J. J. Yellenno, A. Nadasen, R. S. Tickle, and E. Norbeck, Phys. Rev. Lett. **70**, 1924 (1993).
[12] M. B. Tsang *et al.*, Phys. Rev. Lett. **71**, 1502 (1993).
[13] V. Lips, R. Barth, H. Oeschler, S. P. Avdeyev, V. A. Karnaukhov, W. D. Kuznetsov, L. A. Petrov, O. V. Bochkarev, L. V. Chulkov, E. A. Kuzmin, W. Karcz, W. Neubert, and E. Norbeck, Phys. Rev. Lett. **72**, 1604 (1994).
[14] H. E. Fisher, Ann. Phys. (N.Y.) **3**, 255 (1967).
[15] W. Bauer, Phys. Rev. C **38**, 1297 (1988).
[16] P. J. Siemens, Nature (London) **305**, 410 (1983).
[17] *Nuclear Dynamics and Nuclear Disassembly*, edited by J. B. Natowitz (World Scientific, Singapore, 1989), and references therein.
[18] N. T. Porile, A. J. Bujak, D. D. Carmony, Y. H. Chung, L. J. Gutay, A. S. Hirsh, M. Mahi, G. L. Paderewski, T. C. Sangster, R. P. Scharenberg, and B. C. Stringfellow, Phys. Rev. C **39**, 1914 (1989).
[19] L. G. Moretto, Kin Tso, N. Colonna, and G. J. Wozniak, Phys. Rev. Lett. **69**, 1884 (1992), and references therein.
[20] J. Aichelin, Phys. Rep. **202**, 233 (1990), and references therein.
[21] G. Peilert, H. Stöcker, W. Greiner, A. Rosenhauer, A. Bohnet, and J. Aichelin, Phys. Rev. C **39**, 1402 (1989).
[22] S. R. Souza, L. de Paula, S. Leray, J. Nemeth, C. Ngô, and H. Ngô, Nucl. Phys. A **571**, 159 (1994).
[23] T. Maruyama, A. Ohnishi, and H. Horiuchi, Phys. Rev. C **42**, 386 (1990).
[24] A Ono, H. Horiuchi, T. Maruyama, and A. Ohnishi, Phys. Rev. Lett. **68**, 2898 (1992); T. Maruyama *et al.*, Prog. Theor. Phys. **87**, 1367 (1992).
[25] T. C. Sangster, H. C. Britt, D. J. Fields, L. F. Hansen, R. G. Lanier, M. N. Namboodiri, B. A. Remington, M. L. Webb, M. Begemann-Blaich, T. Blaich, M. M. Folwer, J. B. Wilhelmy, Y. D. Chan, A. Dacal, A. Harmon, J. Pouliot, R. G. Stokstad, S. Kaufmann, F. Videbaek, Z. Fraenkel, G. Peilert, H. Stöker, W. Greiner, A. Botvina,

and I. N. Mishustin, Phys. Rev. C **46**, 1404 (1992).
[26] M. Colonna, P. Rouseel-Chomaz, N. Colonna, M. Di Toro, L. G. Moretto, and G. J. Wozniak, Phys. Lett. B **283**, 180 (1992).
[27] S. Leray, C. Ngô, M. E. Spina, B. Remaud, and F. Sebille, Nucl. Phys. A **511**, 414 (1990).
[28] W. A. Friedman, Phys. Rev. C **42**, 667 (1990).
[29] W. Müller, M. Begemann-Blaich, and J. Aichelin, Phys. Lett. B **298**, 27 (1993); M. Begemann-Blaich *et al.*, Phys. Rev. C **48**, 610 (1993).
[30] Y. G. Ma, Ph.D. dissertation, Institute of Nuclear Research, Academia Sinica, 1994.
[31] G. M. Jin *et al.*, in Proceedings of the 3rd International Conference on Nucleus-Nucleus Collisions, Saint-Malo, 1988, Communications P77.
[32] X. Campi, Phys. Lett. B **208**, 351 (1988).
[33] A. D. Panagiotou, M. W. Curtin, H. Toki, D. K. Scott, and P. J. Siemens, Phys. Rev. Lett. **52**, 496 (1984).
[34] D. Cussol, G. Bizard, R. Brou, D. Durand, M. Louvel, J. P. Party, J. Péter, R. Regimbart, J. C. Steckmeyer, J. P. Sullivan, B. Tamain, E. Crema, H. Doubre, K. Hagel, G. M. Jin, A. Péghaire, F. Saint-Laurent, Y. Cassagnou, R. Legrain, C. Lebrun, E. Rosato, R. MacGrath, S. C. Jeong, S. M. Lee, Y. Nagashima, T. Nakagawa, M. Ogihara, J. Kasagi, and T. Motobayashi, Nucl. Phys. A **561**, 299 (1993).
[35] J. P. Bondorf, R. Donangelo, I. N. Mishustin, and H. Schulz, Nucl. Phys. A **444**, 460 (1985).
[36] H. W. Barz, D. A. Cebra, H. Schulz, and G. D. Westfall, Phys. Lett. B **267**, 317 (1991); D. A. Cebra, S. Howden, J. Karn, A. Nadasen, C. A. Ogilvie, A. Vander Molen, G. D. Westfall, W. K. Wilson, J. S. Winfield, and E. Norbeck, Phys. Rev. Lett. **64**, 2246 (1990).
[37] E. Bauge, A. Elmaani, R. A. Lacey, J. Lauret, N. N. Ajitanand, D. Craig, M. Cronqvist, E. Gualtieri, S. Hannuschke, T. Li, B. Llope, T. Reposeur, A. Vander Molen, G. D. Westfall, J. S. Winfield, J. Yee, S. J. Yellenno, A. Nadasen, R. S. Tickle, and E. Norbeck, Phys. Rev. Lett. **70**, 3705 (1993).
[38] For a discussion of the impact of charge conservation, see, e.g., H. R. Jaqaman, A. R. DeAngelis, A. Ecker, and D. H. E. Gross, Nucl. Phys. A **541**, 492 (1992).